AE International – Europe

Atmospheric Environment 38 (2004) 3983–4000

ATMOSPHERIC ENVIRONMENT

www.elsevier.com/locate/atmosenv

Summertime re-circulations of air pollutants over the north-eastern Iberian coast observed from systematic EARLINET lidar measurements in Barcelona

Carlos Pérez[a], Michaël Sicard[b], Oriol Jorba[a], Adolfo Comerón[b], José M. Baldasano[a,*]

[a] *Laboratory of Environmental Modelling, Universitat Politècnica de Catalunya (UPC), Avda. Diagonal 647 10.23, 08028 Barcelona, Spain*

[b] *Department of Signal Theory and Communications, Lidar Group, Universitat Politècnica de Catalunya (UPC), C/ Jordi Girona 1,3., 08034 Barcelona, Spain*

Received 10 November 2003; accepted 12 April 2004

Abstract

Regular aerosol backscatter measurements using an elastic-backscatter lidar were performed from May 2000 to December 2002 in Barcelona (Spain) in the frame of EU EARLINET Project (European Aerosol Research Lidar Network). Vertical profiles retrieved in a regular schedule confirmed the presence of multiple aerosol layers of regional origin above the mixing layer during numerous measurement days. Analysis of the meteorological situation of the corresponding days showed common synoptic regimes, which are typical in summertime around the region. As documented by earlier studies, under strong insolation and weak synoptic forcing, sea breezes and mountain-induced winds develop to create re-circulations of pollutants along the eastern Iberian coast. Layers are formed when aerosols are injected from the mountains into the return flow at various heights and distances from the coast. Aerosol layers can be found above the mixing layer up to 4000 m with variable thickness typically ranged between 100 and 1000 m. The mixing height mainly oscillates between 400 and 800 m asl in periods of maximum insolation. Four selected episodes are analysed combining lidar profiles, radiosoundings and synoptic meteorology information. One of them includes regional re-circulation aerosols at low levels and upper Saharan dust layers. Maximum backscatter coefficients ranged from 1×10^{-6} to 2×10^{-6} $(\mathrm{m\,sr})^{-1}$ at the wavelength of 1064 nm. Assuming a lidar ratio of 30 sr (60 sr for Saharan dust), aerosol optical depths above the mixing layer ranged from 0.016 to 0.073. Detailed mesoscale analysis of one episode is performed by means of high resolution modelling with the PSU/NCAR Mesoscale Model 5 (MM5).

Keywords: Western Mediterranean Basin; Sea-land breeze; Thermal internal boundary layer; Aerosol optical depth; Mesoscale modelling

1. Introduction

The Western Mediterranean Basin (WMB) is surrounded by high coastal mountains and in summer becomes isolated from the travelling lows and their frontal systems, which affect the weather at higher latitudes (Gangoiti et al., 2001). The meteorology and the origin of the air masses arriving at the Iberian Peninsula (IP) are highly influenced by the Azores high-pressure system which is located over the Atlantic Ocean and that intensifies during the warm season inducing

*Corresponding author.
E-mail address: jose.baldasano@upc.es (J.M. Baldasano).

1352-2310/$ - see front matter © 2004 Elsevier Ltd. All rights reserved.
doi:10.1016/j.atmosenv.2004.04.010

very weak pressure gradient conditions all over the region. A number of studies have shown that during this period, layering and accumulation of pollutants such as ozone and aerosols were taking place along the eastern coast of the IP. The European projects MECAPIP; Meso-meteorological Cycles of Air Pollution in the Iberian Peninsula (1988–1991), and RECAPMA; REgional Cycles of Air Pollutants in the Western Mediterranean Area (1990–1992) characterized the meteorological conditions and mesoscale transport mechanisms over the IP and the WMB from experimental campaigns and modelling results. The following processes were documented (Millán et al., 1992, 1996, 1997, 2000, 2002): formation of a thermal low at a peninsular level which forces the convergence of surface winds from the coastal areas towards the central plateau injecting polluted airmasses into the middle troposphere (3.5–5 km-height); strong levels of subsidence over the WMB due to the synoptic Azores anticyclone and the compensation from the thermal low; sea breezes and upslope winds over the coastal and pre-coastal mountains transport coastal pollutants inland while a fraction of these pollutants are injected in their return flows aloft (2–3 km); once in those upper layers pollutants move back towards the sea and compensatory subsidence creates "stratified reservoir layers" of aged pollutants; the next morning the lowermost layers are drawn inland by the sea breeze.

Baldasano et al. (1994), Soriano and Baldasano (1998) and Soriano et al. (2001) combined a numerical approach with an elastic-lidar sounding campaign to study the circulatory patterns of air pollutants over the Barcelona area (North-eastern IP) in a typical summertime situation. Aerosol layers were observed over Barcelona formed by the return flow of the breeze and forcings caused by the nearby coastal and pre-coastal mountains ranges (0.8–2.5 km). The lidar captured as well the development of a thermal internal boundary layer (TIBL). Toll and Baldasano (2000) and Barros et al. (2003) performed photochemical simulations of the Barcelona air basin showing upper air layers of O_3 caused by the reinforcement of the sea breeze in the coastal range by the upslope winds injecting ground air masses above the mixing layer (ML).

Aerosols are emitted along the high-populated coast together with other gaseous pollutants of interest. Traffic is the main source of air pollution in Barcelona (Costa and Baldasano, 1996). Under strong summer insolation most of the NO_x and VOC's emissions are transformed into oxidants, acidic compounds, O_3 and secondary aerosols (Fenger et al., 1998; Beck et al., 1999; European Commission, 1999). Querol et al. (1998) also showed that the load of crustal aerosols in the arid Ebro Basin increases during summer because of soil re-suspension.

In addition to these complex circulatory patterns over the IP, synoptic scale meteorology induces frequent outbreaks of Saharan dust in summer (Rodríguez et al., 2001). Several recent studies (e.g. Jacobson, 2001), indicate that specially over the summer period, the aerosol radiative forcing in the Mediterranean region is among the highest in the world. Aerosol column resolved observations are strongly required. Lidar devices seem to be the most appropriate. They permit a clear separation of optical effects caused by boundary layer aerosols and lofted aerosol plumes on a routine and continuous basis (Müller et al., 2003). The optical power measured by a lidar device is proportional to the aerosol content of the atmosphere. In the last years, great emphasis was put to provide quantitative aerosol properties (aerosol extinction and backscatter coefficients as a function of height) (Bösenberg et al., 2001, 2003). They have also been increasingly used to estimate the mixing layer height (MH), which is required to understand the chemical and physical processes taking place within the ML (Boers et al., 1984; Dupont et al., 1994; Menut et al., 1999; Matthias and Bösenberg, 2002). Over land surfaces in high-pressure regions the ML has a well-defined structure that evolves with the diurnal heating cycle, while in coastal regions with complex orography, mesoscale phenomena as sea-land breezes and mountain-induced winds modify the BL flow generating circulations in conjunction with diurnal heating cycles (Stull, 1988). The structure of the sea-land breeze, the presence of elevated pollution layers and the formation of the TIBL have been studied by lidar in locations such as Los Angeles (U.S.A.) (Wakimoto and McElroy, 1986), Barcelona (Spain) (Soriano et al., 2001) and Akhtopol (Bulgaria) (Kolev et al., 2000; Skakalova et al., 2003). In this context, further research has been carried out in the Barcelona region within the frame of the European Aerosol Research Lidar Network (EARLINET). 21 stations over Europe performed regular lidar measurements from May 2000 to December 2002 on preselected dates, regardless of weather conditions to provide an unbiased database of the horizontal and vertical distribution of aerosols over Europe (Bösenberg et al., 2001). Among other subjects, the network studied air pollution export from the ML promoted by mountains under the rather different conditions of the individual partner stations.

The following sections present and discuss further results from the measurement period focusing on the aerosol lidar profiles obtained during typical regional episodes over the Barcelona area. The paper is organized as follows. A brief description of the orography of the region is presented in Section 2. A description of the EARLINET project and the Barcelona lidar system is given in Section 3. Section 4 lists the main features of the 2-year lidar measurements concerning the regional recirculation episodes. Aerosol lidar observations of 4

characteristic episodes are presented. Meteorological charts, back trajectory analysis and radiosoundings are used to identify and analyse the episodes. Lidar data are discussed in terms of aerosol backscatter coefficient and aerosol optical depth. This analysis is extended, in Section 5, through a high resolution mesoscale numerical simulation of one episode. Discussion and conclusions are presented in Section 6.

2. Orography of the region

Barcelona is located on the shores of the Mediterranean Sea, on the northeastern corner of the IP (Fig. 1). Its location, together with its surrounding orography contributes to the complexity of the dispersion of pollutants in the region. The major orographic features that influence the flows arriving in the Barcelona area are the Pyrenees and the Ebro valley. The Pyrenees range from 2000 to 3000 m, acting as a natural barrier of the flows and producing important orographic forcings into the low troposphere. The Ebro valley has a length of 350 km, channelling the flows from the Cantabric sea to the Mediterranean or viceversa. A first large range of mountains characterizes the eastern Iberian coast with heights between 500 to 3400 m a few kilometres inland. The Barcelona area is dominated by four main features arranged parallel to the coastline: (1) the coastal plain, which comprises an 8-km strip of land between the sea and the first mountain range and which includes most of the cities in the greater urban area of Barcelona; (2) the coastal mountain range whose main peaks are Garraf

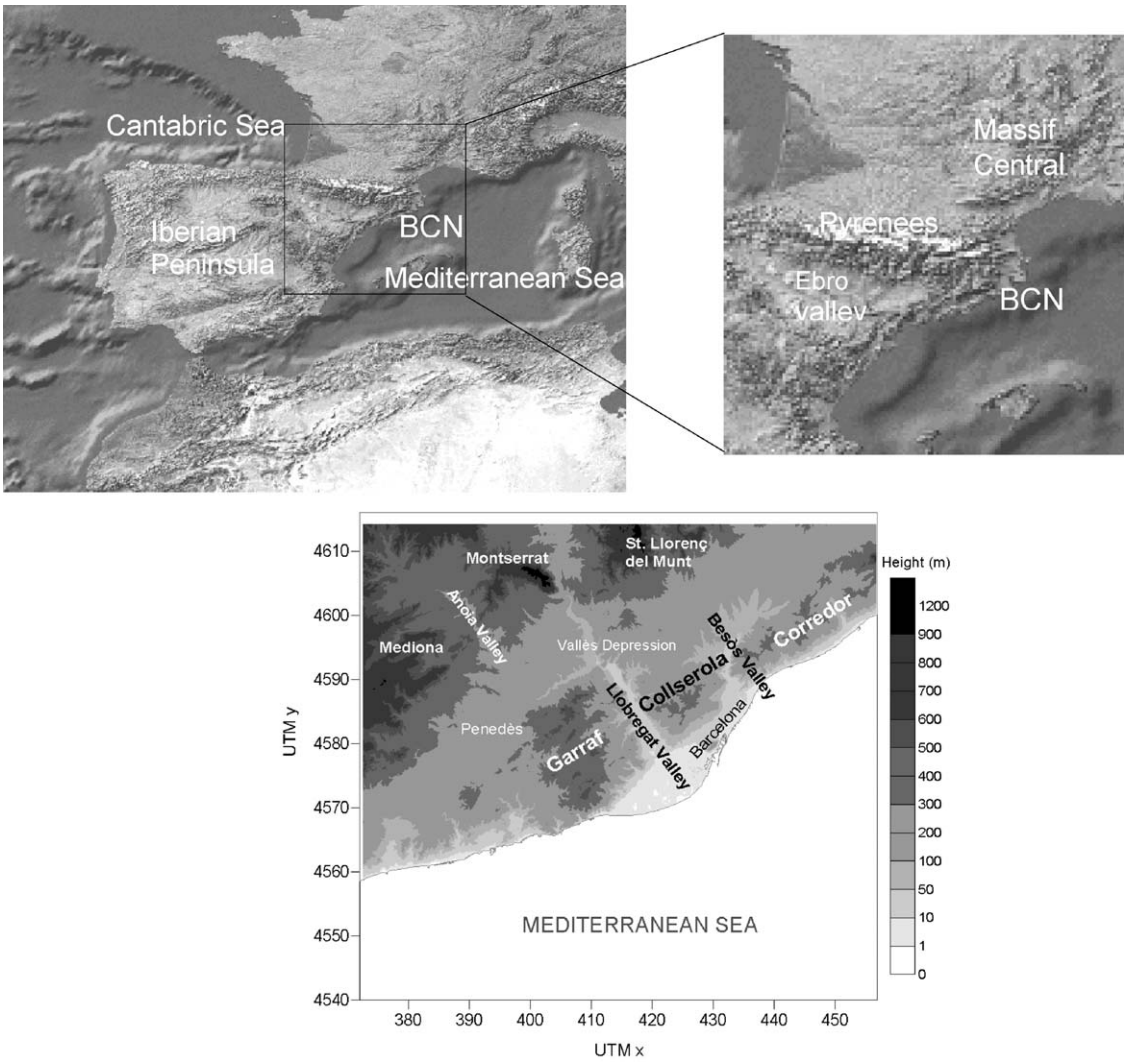

Fig. 1. Location and orography of the Barcelona geographical area.

(594 m), Collserola (512 m) and Corredor (657 m), and (3) the pre-coastal or Vallès depression, situated between the coastal mountain range; and (4) the pre-coastal mountain range, including the mountains of Mediona (744 m), Montserrat (1236 m), St. Llorenç del Munt (1104 m). There are two main river valleys perpendicular to the coast: Llobregat and Besòs. The Llobregat and Besòs valleys contain highways and roads that link Barcelona and its outlying towns with the cities in the Vallès depression. Many industries are located around these urban areas as well as in the above-mentioned valleys.

3. The EARLINET network and the Barcelona aerosol lidar

The EARLINET lidar Network is composed of 21 coordinated stations distributed over most of Europe, using advanced laser remote sensing instruments to measure directly the vertical distribution of aerosols in the troposphere. The main objective of EARLINET, among others, is to establish a comprehensive and quantitative climatological database for the horizontal and vertical distribution and variability of aerosol over Europe. In order to establish a climatological data set it is required that measurements are made under a broad range of meteorological conditions. For this reason a common schedule of three regular measurements a week was agreed. Measurements were performed on Monday at 14:00 LST (local solar time) $+/-1$ h and at sunset -2 h/$+3$ h and on Thursday at sunset -2 h/$+3$ h. The network performed as well diurnal cycle measurements under unperturbed weather conditions, ideally under high-pressure systems to allow simultaneous observations at different stations and quantify the behaviour of aerosol at the regional scale; and observations of special events such as Saharan dust outbreaks.

The aerosol elastic-backscatter lidar system of the Technical University of Catalonia (UPC) (41° 23′ N, 2° 07′ E, 115 m asl) is based on a Nd:YAG laser emitting at 1064 and 532 nm (Rocadenbosch et al., 2001). The range resolution is 7.5 m and, depending on the integration time, useful signal can be obtained from 500 m up to 15000 m asl. The lower limit was reduced in 2002 ($\sim$300 m asl). The lower limit is due to the incomplete overlap between the laser beam and the receiver field of view. Lidar measurements at one wavelength can provide aerosol backscatter profiles using inversion techniques (Klett, 1981; Fernald, 1984). These techniques are generally subject to uncertainties because the lidar system equation contains two unknown parameters, the aerosol extinction and backscatter coefficients, for only one single equation. In order to solve the equation for the aerosol backscatter coefficient, a relationship between the two quantities, the so-called lidar ratio, is assumed. This value has to be guessed and can introduce errors especially in cases with high aerosol optical depth. At the UPC, the most powerful method that was found for single wavelength lidar signal inversion is a combination of the usual Klett (1981) backward method applied with the comments from Fernald (1984) and Sasano and Nakane (1984) in an iterative process. All backscatter coefficient profiles shown in this paper were inverted from lidar signal profiles through this method.

4. Aerosol lidar profiles and synoptic meteorological analysis

The Barcelona EARLINET database comprises 156 valid measurement days from May 2000 to December 2002. The lidar profiles were classified by means of a variety of tools such as back trajectory analysis and synoptic maps. A number of 67 days presented a multi-layer arrangement of aerosols due to regional re-circulations. The meteorological situation around Barcelona was typical of summertime with a weak synoptic situation above the IP and the WMB. In some cases, regional/peninsular re-circulation layers combined with long-range aerosol layers at higher altitudes (e.g. Saharan dust). The percentage of cases (42.9%) is biased mainly because no measurements were performed on rainy days or with low clouds conditions. Furthermore, the measurement period did not cover three entire years (3 summers and 2 winters) and in some cases the system failed or underwent upgrades mainly in winter. Jorba et al. (2004) assessed the frequency of the regional episodes by clustering and classifying into groups of similar length and curvature, five-year kinematic back trajectories computed with the HYbrid Single-Particle Lagrangian Integrated Trajectory model (HYSPLIT) (Draxler and Hess, 1998). The cluster algorithm classified the 1500 m back trajectories into six clusters or groups: northerly flows (N), northwesterly flows (NW), fast westerlies (Fast W), westerlies (W), western re-circulations (wR) and eastern re-circulations (eR). As shown in Table 1, the most dominant situations at low

Table 1
Summary of the cluster results for the 4-days back trajectories arriving at 1500 m asl for the period 1997–2002 (Summer: April to September; Winter: October to March)

Cluster	Total (%)	Summer (%)	Winter (%)
1 N	16	7	9
2 NW	15	6	9
3 Fast W	8	2	6
4 W	15	6	9
5 wR	24	16	8
6 eR	21	13	8

levels in Barcelona are the wR and the eR (45%), especially in summer.

Concerning the ML, the mixing height (MH) was estimated by applying the Inflection Point Method (Sicard et al., 2003) to the lidar profiles during the period of maximum insolation (from 1000 to 1500 UTC), which corresponds to the unstable thermal stratification. Fig. 2 shows the MH in Barcelona retrieved by the IPM over the period 2000–2002 from April to September. The majority of the estimated heights oscillate between 400 and 800 m asl, in contrast to continental regions where the MH can overpass 2000 m asl in summer (Bösenberg et al., 2003).

In this section, four episodes are selected from the Barcelona EARLINET database and discussed together with meteorological synoptic charts, 4-day atmospheric back trajectory analysis and radiosoundings. Lidar backscatter coefficient profiles at 1064 nm are integrated over 30 min. The respective extinction coefficients are estimated by multiplying the backscatter coefficients by the lidar ratio of 30 sr. The integration of the extinction coefficient from the ML top through the atmospheric column yields the aerosol optical depth (AOD) of the re-circulation layers. Synoptic charts were produced with the ARLPLOT—Meteorological Mapping of the NOAA Air Resources Laboratory using the FNL data product. Radiosoundings are presented as vertical profiles of wind direction and relative humidity. The MH estimation from this data is done by means of the Richardson number method considering a critical bulk Richardson number of 0.21. All heights are expressed in altitude above sea level (asl). Back trajectories were calculated by the German Weather Service (DWD) for the EARLINET Barcelona station for four arrival pressure levels (975, 850, 700, 500 hPa, which are equivalent to the ML height range, 1500, 3000, and 5500 m, respectively) and two arrival times per day (1300 and 1900 UTC). The latter correspond approximately to the times of the routine lidar observations at noon and at sunset. Back trajectories were calculated on a 3-dimensional grid. This calculation method leads to lower uncertainties in comparison to those from other methods, e.g. isentropic calculation. The accuracy of the calculated trajectories also depends on synoptic conditions. Higher wind speeds are generally associated to lower trajectory errors. Synoptic back trajectories associated to regional episodes do not represent the detailed movement of the air masses. Mesoscale effects may not be captured by the analyses from which the trajectories are calculated but nevertheless they represent a useful tool to identify and analyse situations where these mesoscale effects should develop (Rodríguez et al., 2002; Jorba et al., 2004).

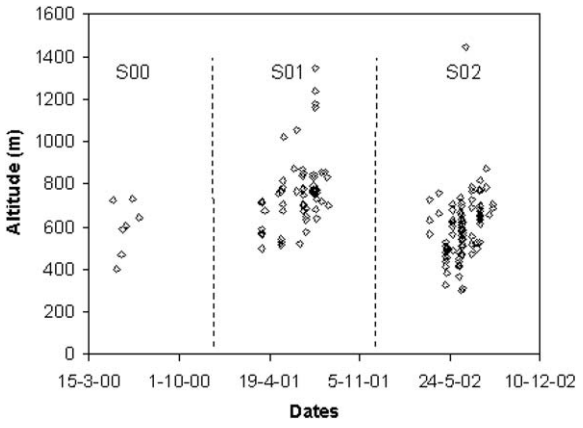

Fig. 2. Mixing layer height in summer derived from lidar measurements as a function of day between 2000 and 2002.

4.1. 14 August 2000

An intense episode of photochemical air pollution was produced from 10 to 19 August 2000 in the northeastern IP. The highest ozone level of the year was reached in this region with a maximum hourly mean of 273 $\mu g\,m^{-3}$ on 15 August. During this period the PM_{10} and O_3 daily mean concentrations ranged between 20 and 40 $\mu g\,m^{-3}$ and between 100 and 150 $\mu g\,m^{-3}$, respectively (Rodríguez et al., 2002). The more intense part of the episode covered days 14 to 16. From 10 August, a very weak pressure gradient covered the whole Mediterranean Basin and central Europe. A thermal low developed over the IP which persisted throughout the episode (Fig. 3d). The relative high pressure area over the WMB associated with large mesoscale sinking (Millán et al., 1992) is clearly observed from the analysis. On 14 August, between 1435 and 1505 UTC the low troposphere showed multiple layers above the ML (Fig. 3a) at 700–800, 1150–1250, 1600–2300 and 2400–3500 m with a maximum backscatter coefficient of 3×10^{-7} $(m\,sr)^{-1}$ at 2800 m and an AOD of 0.020. The MH was located at 565 m. From 1827 to 1857 UTC (Fig. 3b) the MH decreased to 547 m and upper aerosol layers were present up to 4000 m with similar AOD values (0.019). The 4-day synoptic back trajectory analysis (Fig. 3e) outlines the stagnant conditions during the period 10–14 August. Air masses arriving from the south in the ML (975 hPa) at 1300 UTC had previously circulated over the WMB for at least 4 days, while the upper levels (700 and 850 hPa) showed a peninsular origin arriving over Barcelona from W to NW directions. It is remarkable the injection of air masses from 900 hPa at the northern Iberian coast and their slow circulation over the IP before reaching Barcelona at 700 hPa. Compensatory subsidence from the large mesoscale circulation may explain the final drop of back trajectories (Millán et al., 1992). The steep reduction on the relative humidity profile at 12 UTC (from nearly 50 to 30%) below 1000 m

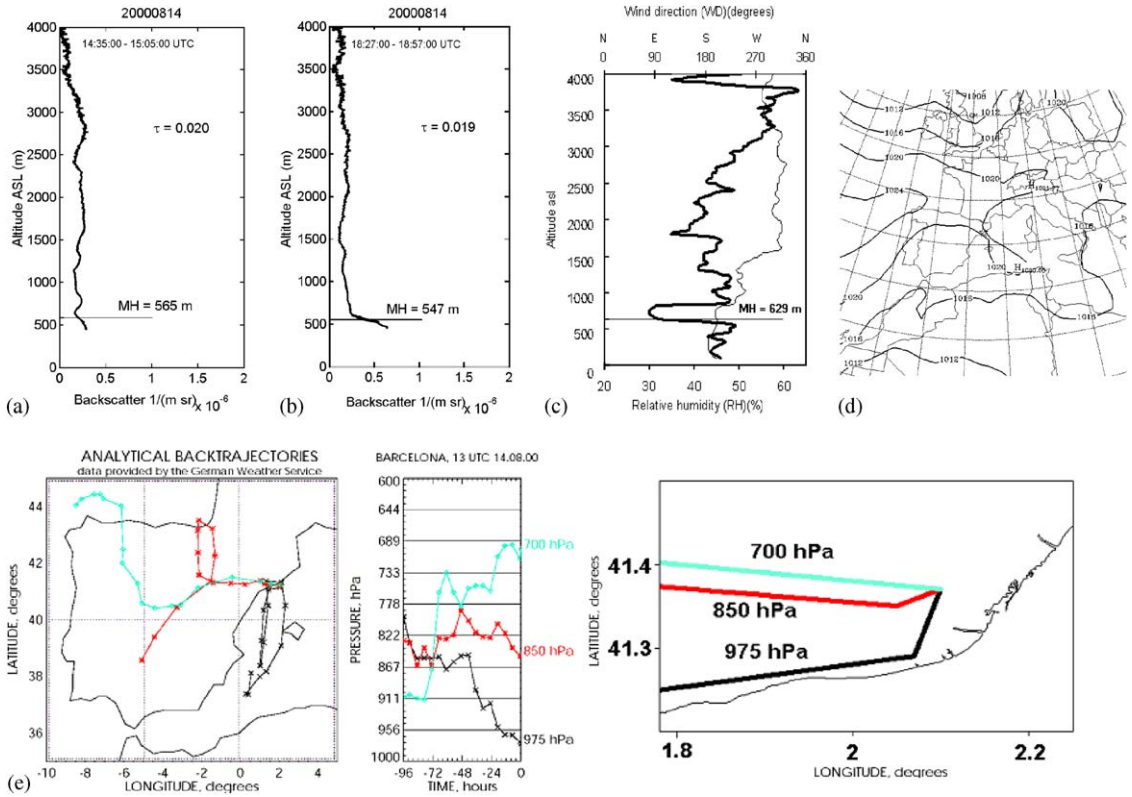

Fig. 3. Plots for the 14 August 2000. (a) 1064 nm backscatter coefficient profile from 1435 to 1505 UTC. (b) 1064 nm backscatter coefficient profile from 1827 to 1857 UTC. The horizontal line indicates the mixing height derived from the Inflection Point Method. Aerosol optical depth values (τ) are calculated from the respective column backscatter values multiplied by a lidar ratio of 30 sr. (c) Radiosounding profile at 12 UTC. Thick solid line shows relative humidity (%). Thin solid line shows wind direction (degrees). The horizontal line indicates the mixing height derived from the Richardson number Method. (d) MSL pressure at 1800 UTC. (e) (left) 4-day back trajectories for arrival pressures of 700, 850 and 975 hPa at 13 UTC and (right) zoom of the arrival.

indicates the ML top (Fig. 3c). The Richardson number methods yields a MH of 629 m which is consistent with the lidar-derived MH at 1435–1505 UTC. Arrival directions of the back trajectories are also confirmed by the radiosounding in Fig. 3c: southern sea-breeze flows up to 800 m, SW flows from 900 to 1500 m and W-NW flows from 1600 to 4000 m. Under such sea breeze conditions, a TIBL may be formed as previously observed by Soriano et al. (2001). The aerosol layers observed up to 1500 m may be formed by the return flow of the breeze and forcings caused by the nearby coastal and pre-coastal mountains ranges. High resolution modelling of this episode in Section 5 shows the local mesoscale details of these flows which account for the lower layers detected by the lidar.

4.2. 19–21 June 2001

The surface pressure map on 19 June 2001 (Fig. 4d) features the influence of the southern edge of a high pressure system located over northwestern Europe inducing weak pressure gradient conditions over the region, and the formation of the typical Iberian thermal low with its correspondent relative high pressure area above the WMB (Millán et al., 1992). In the afternoon the lidar detected several high loaded aerosol layers up to 3500 m (Figs. 4a–c). The MH from 1334 UTC to 1404 UTC was located at 874 m (Fig. 4a) which is consistent with the radiosounding at 12 UTC (Fig. 4e) that yields a MH of 788 m. Relative humidity values seem to correlate well with backscatter coefficients up to 2000 m. Humidity effects can be important on the lidar data through a swelling of the aerosols and an increase of its effective cross section. This correlation was already outlined by Soriano et al. (2001) and may explain the raise of backscatter coefficients within the ML (see Figs. 4a–e). Two aerosol layers were clearly distinguished above the ML at 1000–1300 and 1400–2200 m with a maximum backscatter coefficient of 1×10^{-6} $(\mathrm{m\,sr})^{-1}$ at 1150 m. The AOD reached 0.029. The MH from 1541 to

1611 UTC descended to 771 m (Fig. 4b) and the first elevated layer was located at 900–1100 m with a decreased backscatter coefficient of 3×10^{-7} $(\mathrm{m\,sr})^{-1}$. An additional layer appeared above the 1400–2200 m layer up to 3000 m. The AOD raised up to 0.033. Finally, from 1728 to 1758 UTC (Fig. 4c), the MH descended to 583 m and the aerosol content significantly decreased below 1400 m. The backscatter coefficient of the highest layer raised to a maximum of 6×10^{-7} $(\mathrm{m\,sr})^{-1}$ around 2900 m and the AOD slightly increased to 0.034. Fig. 4f outlines that the back trajectories arriving at 1900 UTC originated over the UK 4 days before. The 975 hPa back trajectory originated around 700 hPa, crossed the Pyrenees dropping over the Mediterranean Sea due to generalized and compensatory subsidence (see Fig. 4d), and circulated for at least 1 day before reaching the coastline. The 850 hPa back trajectory captures the sea-breeze flows over the coast on 18 June and injections from the Tarragona coastal mountains (southwest of Barcelona) into the return flows that finally arrive over Barcelona from the NW-N. The lidar profile in Fig. 4c shows a dense layer at those

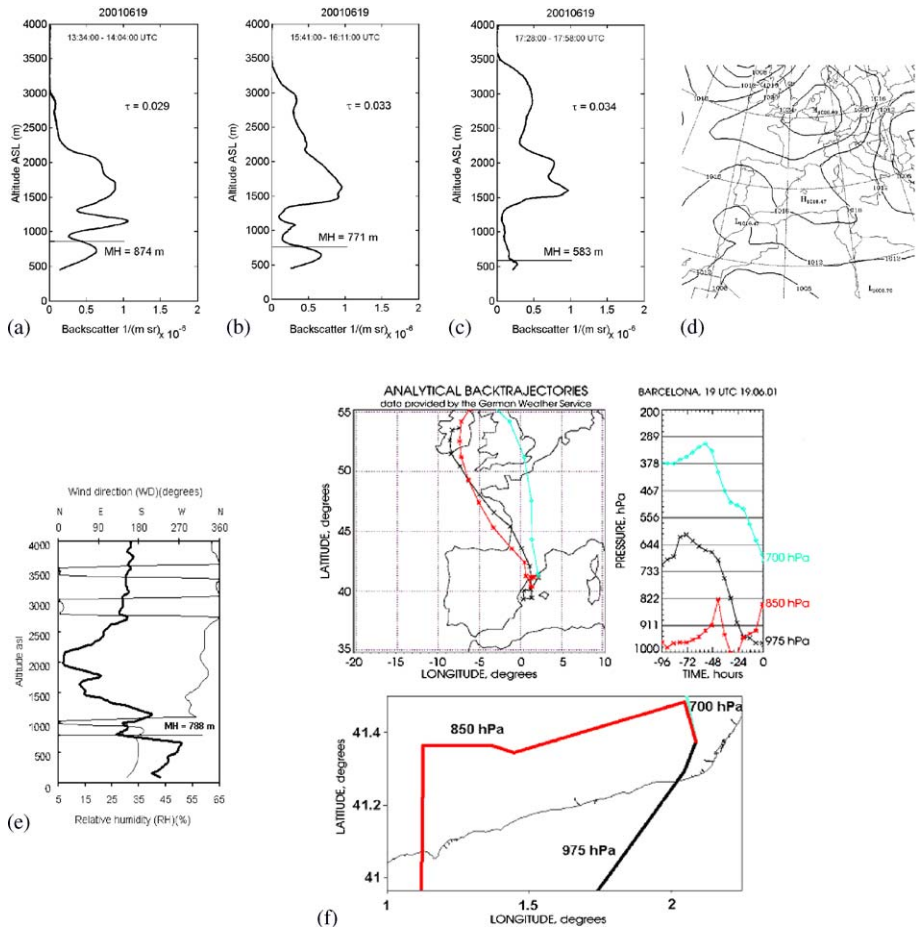

Fig. 4. Plots for the period 19–21 June 2001. (a) 1064 nm backscatter coefficient profile from 1334 to 1404 UTC on 19 June. (b) 1064 nm backscatter coefficient profile from 1541 to 1611 UTC on 19 June. (c) 1064 nm backscatter coefficient profile from 1728 to 1758 UTC on 19 June. The horizontal line indicates the mixing height derived from the Inflection Point Method. Aerosol optical depth values (τ) are calculated from the respective column backscatter values multiplied by a lidar ratio of 30 sr. (d) MSL pressure at 1800 UTC on 19 June. (e) Radiosounding profile on 19 June at 12 UTC. Thick solid line shows relative humidity (%). Thin solid line shows wind direction (degrees). The horizontal line indicates the mixing height derived from the Richardson number Method. (f) (top) 4-day back trajectories for arrival pressures of 700, 850 and 975 hPa on 19 June at 19 UTC and (bottom) zoom of the arrival. (g) 1064 nm backscatter coefficient profile from 0842 UTC to 0912 UTC on 20 June. (h) 1064 nm backscatter coefficient profile from 1646 to 1716 UTC on 20 June. (i) 4-day back trajectories for arrival pressures of 700, 850 and 975 hPa at 13 UTC on 20 June. (j) 1064 nm backscatter coefficient profile from 1830 to 1900 UTC on 21 June. (k) MSL pressure at 0600 UTC on 21 June. (l) 4-day back trajectories for arrival pressures of 700, 850 and 975 hPa at 19 UTC on 21 June.

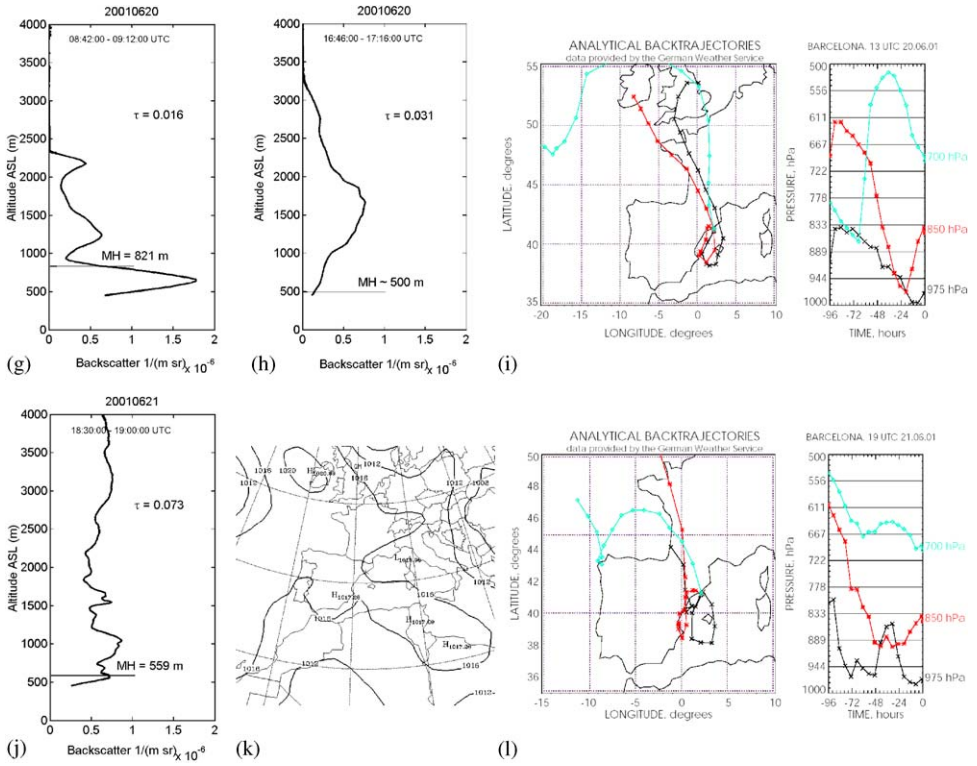

Fig. 4 (*continued*).

heights (1500–2000 m). The 700 hPa back trajectory indicates that the upper layer detected above 2200 m may be the result of long range transport. The arrival direction of the back trajectories is supported by the wind direction profile in Fig. 4e. On 20 June similar synoptic conditions persisted (not shown). In the morning, from 0842 to 0912 UTC the MH was located at 821 m and two layers remained above with peaks at 1200 and 2150 m reaching a maximum backscatter coefficient of 1.8×10^{-6} $(\mathrm{m\,sr})^{-1}$ (Fig. 4g) and lower AOD values (0.016). In the afternoon from 1646 to 1716 UTC, the atmosphere was loaded up to 3200 m with highest backscatter coefficients (3×10^{-7}–7×10^{-7} $(\mathrm{m\,sr})^{-1}$) between 1000 and 2000 m (Fig. 4h). The MH could not be derived from the lidar profile. Two reasons are possible given that the radiosounding profile (not shown) yielded a MH of 647 m at 12 UTC: either the ML was coupled to the upper layer in terms of backscatter coefficient or the MH was below the detection limit of the lidar (500 m). In order to calculate the AOD (0.031) a MH of 500 m was considered. Back trajectory analysis shows a similar pattern to the previous day (Fig. 4i). The air masses came from the north, crossed the Pyrenees and dropped to the Mediterranean Sea where they circulated for 2 days before reaching Barcelona. As observed in the previous case, the 850 hPa back trajectory may indicate that aerosols were injected from the coastal mountains into the return flows sinking before their arrival due to generalized and compensatory subsidence. On 21 June at 0600 UTC, the high pressure center over northwestern Europe had moved northeast and a relative high pressure system established over the WMB (Fig. 4k). The Iberian thermal low developed throughout the day. From 1830 to 1900 UTC the lidar captured a multi-layer aerosol enriched atmosphere up to at least 4000 m with backscatter coefficients ranging from 5×10^{-7} to 7×10^{-7} $(\mathrm{m\,sr})^{-1}$ (Fig. 4j) reaching a high AOD (0.073). Fig. 4l features the circulations over 3 days of the air masses arriving at 850 and 975 hPa with injections from the coastal mountains. The 700 hPa backtrajectory indicates the possible aerosol enrichment of the air masses 3 days before over the northwestern IP by the effect of the Iberian Thermal low that raises up the pollutants into high levels (Millán et al., 1992)

4.3. 2 July 2001

On 2 July 2001 the Azores high pressure system extended over northwestern Europe and the Mediterra-

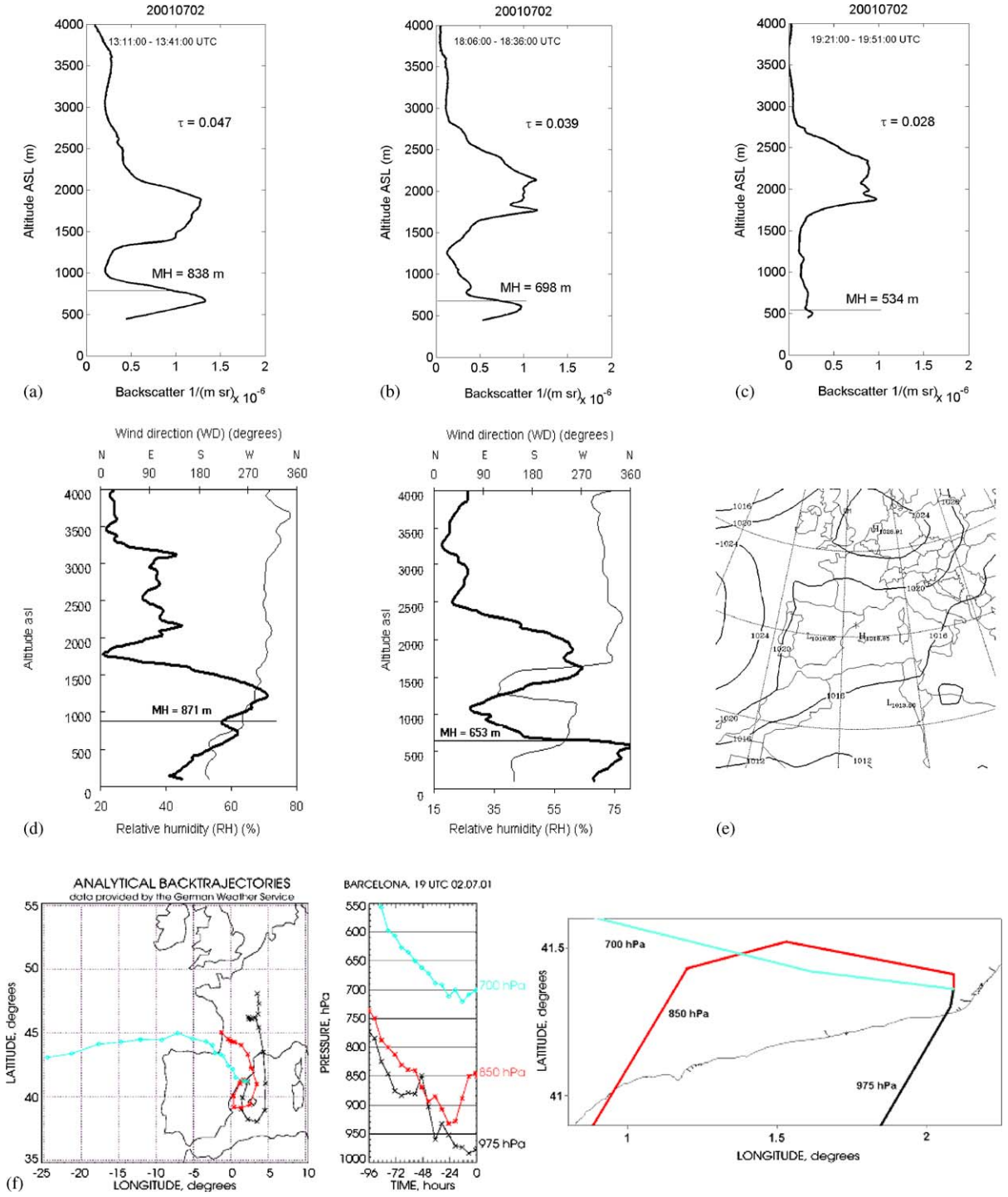

Fig. 5. Plots for the 2 July 2001. (a) 1064 nm backscatter coefficient profile from 1311 to 1341 UTC. (b) 1064 nm backscatter coefficient profile from 1806 to 1836 UTC. (c) 1064 nm backscatter coefficient profile from 1921 to 1951 UTC. The horizontal line indicates the mixing height derived from the Inflection Point Method. Aerosol optical depth values (τ) are calculated from the respective column backscatter values multiplied by a lidar ratio of 30 sr. (d) (left) Radiosounding profile at 12 UTC and (right) radiosounding profile at 18 UTC. Thick solid line shows relative humidity (%). Thin solid line shows wind direction (degrees). The horizontal line indicates the mixing height derived from the Richardson number Method. (e) MSL pressure at 1800 UTC. (f) (left) 4-day back trajectories for arrival pressures of 700, 850 and 975 hPa at 19 UTC and (right) zoom of the arrival.

nean Basin. As in the previous case, the surface isobars feature a weak pressure gradient above the eastern Iberian coast and the formation of the Iberian Thermal low with its compensatory relative high pressure region over the sea (Fig. 5e). Back trajectories arriving at 850 and 975 hPa at 1900 UTC confirm the slow speeds and the anticyclonic curvature of the air masses at low levels (Fig. 5f) while the flow arriving at 700 hPa showed a northwestern direction. From 1311 to 1341 UTC the MH was located at about 838 m (Fig. 5a) which is supported by the MH derived from the radiosounding profile at 12 UTC (Fig. 5d left). The troposphere was loaded up to 4000 m with a clear defined layer coming from the northwest at 1300–2200 m (see radiosounding in Fig. 5d left) and showing high backscatter coefficients (up to 1.3×10^{-6} (m sr)$^{-1}$) with an AOD of 0.047. From 1806 to 1836 UTC the MH had descended to 698 m (Fig. 5b). The reduction of the basckscatter coefficient in the range 3000–4000 m accounts for the drop of the AOD (0.039). The radiosounding at 18 UTC (Fig. 5d right) confirms again the MH retrieved from the lidar profile ($\sim$653 m) and the high correlation between backscatter coefficients and relative humidity values as discussed in Section 4.2. Back trajectory analysis at 19 UTC (Fig. 5f) at 850 hPa points out the air mass injections at the eastern Iberian coast (over Tarragona) with arrival from the northwest over Barcelona. From 1921 to 1951 UTC the ML height decreased to 534 m (Fig. 5c). The aerosol content was significantly reduced below 1500 m and above 3000 m and the AOD dropped to 0.028.

4.4. 14 June 2002

On 14 June 2002 the IP was framed by the Azores high on the southwest and a relative high pressure area extending over Europe and the Mediterranean while the typical Iberian thermal low developed due to the high temperatures reached over the Spanish Plateau (Fig. 6e). For this day, the lidar carried out a diurnal cycle measurement. A height-time display (60 s temporal resolution) of the 1064 nm range-corrected signal (arbitrary units) is shown in Fig. 6a. Dark blue columns show the periods with no measurements. Two differentiated aerosol structures are detected by the lidar: plume-like structures from 3500 to 5500 m (in the afternoon) with traces of aerosol up to 7000 m and a more stratified structure below 3000 m throughout the day. Back trajectory analysis clearly identifies the Saharan origin of the upper plume-like structures (Fig. 6g). The 500 hPa back trajectory was injected by convection over the Saharan region at near ground levels and transported towards the IP. This is supported by the geopotential height chart at 500 hPa on 13 June at 18 UTC that features the cyclonic curvature of the 5880 m geopotential line inducing southern winds over the IP from North Africa (Fig. 6f). DREAM dust model (Nickovic et al., 2001) simulations for that day show the presence of Saharan dust over the northeastern Iberian coast (not shown).

The lower stratified layers are the result of regional recirculations. Fig. 6b shows the integrated backscatter profile from 1120 to 1150 UTC which indicates a MH of 438 m. This is supported by the radiosounding at 12 UTC that yields a MH of 523 m (Fig. 6d). Three layers are detected above the ML and below 3000 m (at 600–1100; 1200–1600; 1800–3000m). The lowest one comes from the west (see wind profile in Fig. 6d). This strongly suggests that the aerosols detected at this height may have been injected from the Garraf mountain (see Section 2 and Fig. 1) into the return flow. The wind profile of the radiosounding at 12 UTC and back trajectories at 19 UTC show that the stratified layers between 1200 and 3000 m arrive from the south-southwest with compensatory subsidence suggesting the entry of aged pollutants from the WMB. The MH decreases during the afternoon to a value of 311 m at 1758–1828 UTC (Fig. 6c).

A lidar ratio of 60 sr was used for Saharan dust (Figs. 6b and c). This value seems to be the most appropriate after long range transport to western and northern Europe (Mattis et al., 2002; Müller et al., 2003; Ansmann et al., 2003). At noon most of the AOD (0.047) was due to the re-circulation layers below 3000 m while in the afternoon Saharan dust was dominant (AOD = 0.046).

5. Mesoscale modelling on 13–15 August 2000

In order to have a detailed picture of the local mesoscale processes that contribute to the formation of the re-circulation layers frequently detected by the lidar, a numerical simulation was run with the PSU/NCAR Mesoscale Model 5 (MM5), version 3, release 4 modeling system (Dudhia, 1993; Dudhia et al., 2004), for the period 13–15 August 2000, which covers the episode presented in Section 4.1. MM5 is a community non-hydrostatic mesoscale primitive equation model widely used for numerical weather prediction, air quality, and hydrological studies.

Four nested domains were selected (Fig. 7), which essentially covered Europe (Domain 1, D1), the IP (Domain 2, D2), the northeastern IP (Domain 3, D3) and the Catalonia area (Domain 4, D4). D1 is formed by 35×50 grid points in the horizontal with 72-km grid-point spacing; D2, 61×49 24-km cells; D3, 93×93 6-km cells; and D4, 151×151 2-km cells. A one-way nesting approach was used. The vertical resolution was of 29 σ-layers for all domains, the lowest one situated approximately at 10 m AGL and 19 of them below 1 km agl. The upper boundary was fixed at 100 hPa. Initialization and boundary conditions were introduced with analysis data

of the ECMWF global model. Data at 1° resolution were available (100-km approx. at the working latitude) at the standard pressure levels every 6 h. The physics options used for the simulations were: the Mellor–Yamada scheme as used in the Eta model (Janjic, 1994) for the PBL parameterization, the Anthes–Kuo and Kain–Fritsch cumulus scheme (Kain and Fritsch, 1993), the Dudhia simple ice moisture scheme, the cloud-radiation scheme, and the five-layer soil model (MMD/NCAR, 2001). Comparisons with measurements were done in order to evaluate the reliability of the model results, and to validate the model under weak synoptic conditions over the IP. Reasonable agreement was produced between model results and observations (Jorba et al., 2003).

5.1. Model results

As previously noted in Section 4.1, the IP was dominated by the Azores anticyclone, with very low pressure gradients. The sea-breeze regime, developed within all the western Mediterranean coast, induced an anticyclonic circulation over all the WMB with general and compensatory subsidence over the region (Millán et al., 1992). Fig. 8a shows the surface streamlines at 0600 UTC on 14 August. The maintenance of the anticyclonic circulation over the WMB at this time from the previous day (not shown) is remarkable. The whole eastern Iberian coast presented down-slope winds over the mountains and general offshore breeze flows. The canalization between the Pyrenees and the Central Massif introduced northwestern flows into the Mediterranean. At low levels, this canalization plays an important role, because it is the only pass bringing fresh air into the WMB (Gangoiti et al., 2001).

As the day advanced, a well developed sea-breeze regime established along all the eastern Iberian coast with breeze circulation cells up to 2000 m height. This regime covered the central hours of the day, starting around 0800–1000 UTC and changing to land-sea flows around 1900 UTC. Fig. 8b shows the surface streamlines at 1800 UTC on 14 August. The onshore winds are well developed along all the eastern coast, intensifying the anticyclonic circulation and deflecting to the east the flow between the Pyrenees and the Central Massif. The deflection of this flow is a frequent feature in summer as showed by Gangoiti et al. (2001). Fig. 8b also outlines the high temperatures reached over the IP during the day, which strongly suggests the development of a thermal low over the Spanish Central Plateau as previously noted by Millán et al. (1992), and the formation of a thermal mesolow over the arid Ebro Valley (Tudurí et al., 2003), causing low level convergence and ascent. These peninsular scale features may be involved in the formation of the elevated pollutant layers (3000–4000 m) detected by the lidar (see Fig. 3e: the 700 hPa back trajectory comes from the centre of the IP 2 days before).

The strength of the sea breeze and the complex orography of the eastern Iberian coast produce several injections due to orographic forcing. Two north-to-south vertical cross sections of the wind field, the potential temperature and the mixing ratio over the domain D4 as indicated in Fig. 9, are displayed in Fig. 10 in order to view the air mass injections. Cross section A covers the coastal plain which comprises the Tarragona area (100 km southwest from Barcelona), a first mountain range (Prades mountains) reaching an altitude of 1000 m, the central depression, the Montsec mountain range (~1000 m) and the Pyrenees (~3000 m). Cross section b covers, as described in Section 2, a coastal plain which includes the Barcelona area, the Collserola mountain (~500 m), the pre-coastal depression, the St. Llorenç del Munt mountain (~1000 m), the central plain and the Pyrenees (~3000 m). Fig 10a shows the development of the typical daytime flows characterized by an onshore sea breeze and up-slope mountain winds. As the sea breeze front advances inland reaching the mountain ranges, orographic injections occur at different altitudes. At 1100 UTC, the breeze has reached the first mountainous chain producing upward motions up to 2500 m. Fig. 10b features the situation at 1600 UTC in cross section b. At this time of the day, the sea-breeze front has passed over the coastal mountain range and reached the central plain (~100 km from the coast), overwhelming the upslope winds in the opposite direction. Strong thermally driven convections appear at the central plain injecting air masses up to 3000–4000 m. The mixing ratio allows the visualization of the return flows to the sea.

In order to explain the origin and local pathways of the polluted air masses producing some of the elevated layers detected by the lidar up to 1500 m, the HYSPLIT trajectory model (Draxler and Hess, 1998) was used to calculate some representative kinetic back trajectories from the MM5 D4 simulation at the times of the lidar measurements (1500 and 1900 UTC) on 14 August. Fig. 11 (left) plots 4 representative back trajectories arriving over the lidar station at 1500 UTC between 500 and 1500 m. The sea breeze entrance at low levels is clearly depicted by the 3-h back trajectory arriving at 525 m. The 15-h back trajectories arriving at 933 m (blue) and 1464 m (red) outline the channelling of air masses along the pre-coastal depression at ground levels from 0000 to 0500–0700 UTC, due to the persistence of the anticyclonic circulation over the WMB as previously mentioned. From 0500 to 0800 UTC the blue trajectory follows the offshore drainage flows through the Llobregat Valley and at 0900–1000 UTC it is injected from the Garraf mountain up to 1300 m by the sea breeze and the up-slope winds. Some air was channelled through

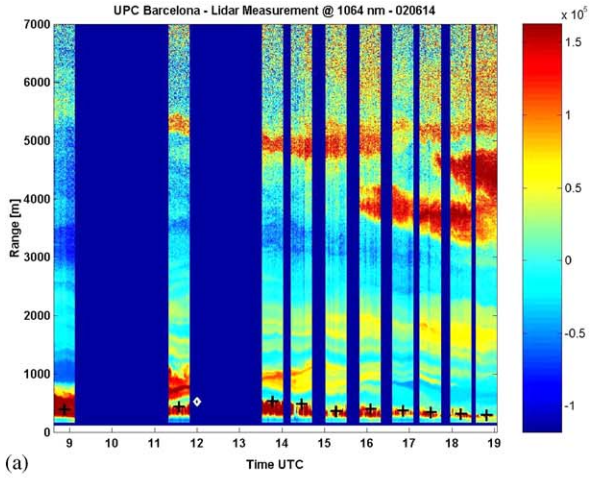
UPC Barcelona - Lidar Measurement @ 1064 nm - 020614
Range [m]
Time UTC
x 10^5

(a)

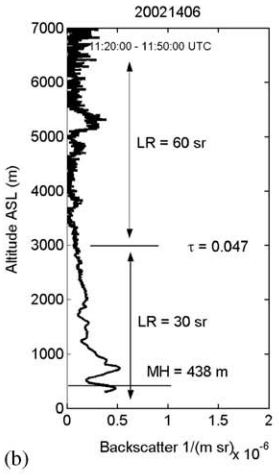
20021406
11:20:00 - 11:50:00 UTC
LR = 60 sr
τ = 0.047
LR = 30 sr
MH = 438 m
Altitude ASL (m)
Backscatter 1/(m sr) x 10^-6

(b)

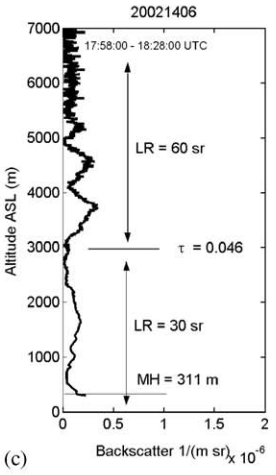
20021406
17:58:00 - 18:28:00 UTC
LR = 60 sr
τ = 0.046
LR = 30 sr
MH = 311 m
Altitude ASL (m)
Backscatter 1/(m sr) x 10^-6

(c)

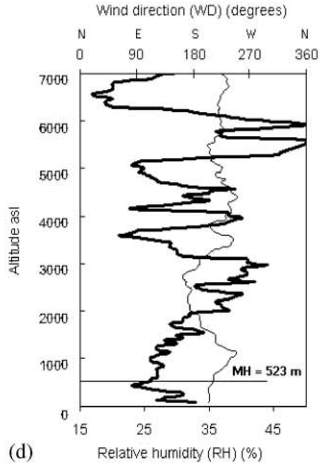
Wind direction (WD) (degrees)
N E S W N
0 90 180 270 360
Altitude asl
MH = 523 m
Relative humidity (RH) (%)

(d)

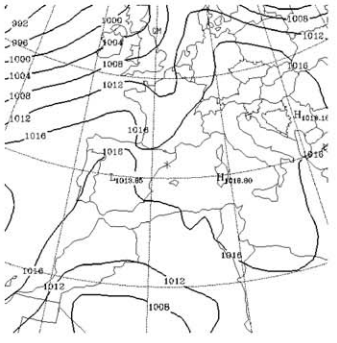

(e)

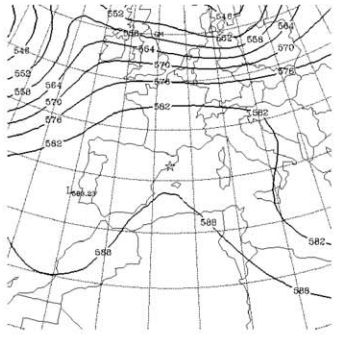

(f)

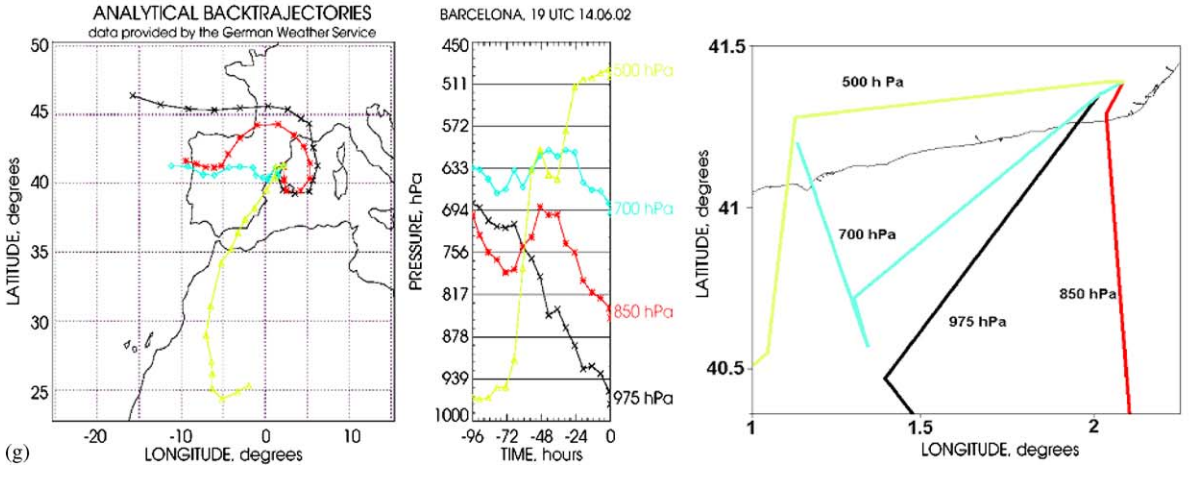
ANALYTICAL BACKTRAJECTORIES
data provided by the German Weather Service
LATITUDE, degrees
LONGITUDE, degrees
BARCELONA, 19 UTC 14.06.02
PRESSURE, hPa
TIME, hours
500 hPa
700 hPa
850 hPa
975 hPa
500 h Pa
700 hPa
850 hPa
975 hPa
LATITUDE, degrees
LONGITUDE, degrees

(g)

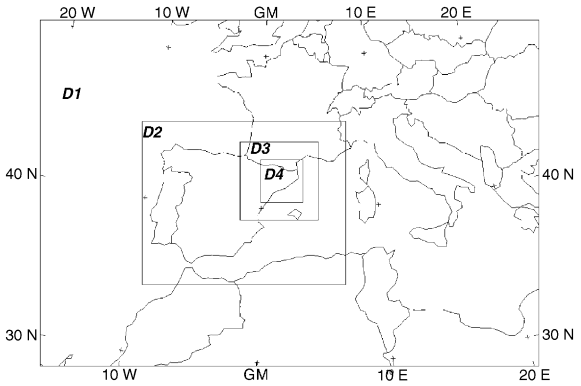

Fig. 7. Four-nested domain configuration. D1: 35×50 72-km cells. D2: 61×49 24-km cells. D3: 93×93 6-km cells. D4: 151×151 2-km cells.

the Anoia Valley and around 1000–1100 UTC it was lifted from the Montserrat mountain up to 2200 m. From 1200 to 1500 UTC, the rising air returned to the coast. Compensatory subsidence is induced in the return flow. The 15-h back trajectory arriving at 1233 m (green) originates over the pre-coastal mountain range and follows the weak nocturnal offshore regime, reaching the coastline by 0900 UTC. At this time, the sea breeze propagated inland through the Llobregat Valley. By 1200 UTC the air was lifted at the southern slope of the St. Llorenç del Munt mountain up to 1500 m from where it returned to the coast dropping by compensatory subsidence to 1233 m. Fig. 11 (right) plots representative back trajectories arriving over the lidar station at 1900 UTC between 500 and 1500 m asl. As depicted by the blue and red trajectories, some air masses were transported from 0000 to 0500 UTC along the coast and then circulated at ground levels over the Mediterranean Sea owing to the offshore flows and the subsequent transition to onshore flows. The green trajectory shows the channelling of air from the pre-coastal mountain range to the coastal plain through the main valleys between 0000 and 0900 UTC. Air injections are produced at the Garraf mountain and the Montserrat mountain up to at least 1300 and 2100 m, respectively, with later return over Barcelona sinking by compensatory subsidence. Once in low levels over the Mediterranean some air masses may re-circulate over the sea with a possible return to the coast on the next days.

6. Discussion and conclusions

Systematic lidar measurements from May 2000 to December 2002 in the frame of the EU EARLINET Project have shown the vertical aerosol structure of the low to middle troposphere during a recurrent summer weather regime in the region: the absence of large scale forcing due to the establishment of weak pressure gradients and the development of mesoscalar flows related to the daily heating and cooling cycle (sea-land breezes, mountain-induced winds, valley winds and thermal lows) that create regional re-circulations of pollutants over the eastern Iberian coast. From 156 valid measurement days, 67 days presented a multi-layer structure of aerosols due to regional re-circulations. Aerosol layers can be found above the ML up to 4000 m with variable thickness typically ranged between 100 and 1000 m. The MH mainly oscillates between 400 and 800 m during the period of maximum insolation, in contrast to other continental areas where the MH can overpass 2000 m in summer (Bösenberg et al., 2003). The average MH in summer is smaller than the average MH in winter (Sicard et al., 2003). In summer, several phenomena interact at various scales driving the ML evolution over Barcelona. Sea-breeze flows generate a TIBL over the city as observed by Soriano et al. (2001). The physical processes that govern the development of the thermal internal boundary layer are mechanically and thermally generated turbulent kinetic energy within the layer, entrainment and subsidence aloft and mesoscale advection through the layer (Batchvarova et al., 1999). Generalized subsidence due to the Azores anticyclone and compensatory subsidence from the Iberian thermal low over the WMB represent the synoptic and large mesoscale phenomena that may explain the small growth of the ML. Millán et al. (1992, 1997) have documented the first rapid rise of the MH during the

Fig. 6. Plots for the 14 June 2002. (a) Range corrected 1064 nm signal (arbitrary units) between 0838 and 1904 UTC (temporal resolution is 60 s). Dark blue columns indicate no measurements. Blue colors indicate weak backscattering and yellow and red colors indicate higher backscattering. Black crosses indicate the mixing height derived from the Inflection Point Method. The white diamond indicates the mixing height from the radiosounding at 12 UTC. (b) 1064 nm backscatter coefficient profile from 1120 to 1150 UTC. (c) 1064 nm backscatter coefficient profile from 1758 to 1828 UTC. The horizontal line indicates the mixing height derived from the Inflection Point Method. Aerosol optical depth values (τ) are calculated from the respective column backscatter values multiplied by a lidar ratio of 30 sr (re-circulation layers) and 60 sr (Saharan dust layers) (d) Radiosounding profile at 12 UTC. Thick solid line shows relative humidity (%). Thin solid line shows wind direction (degrees). The horizontal line indicates the mixing height derived from the Richardson number Method. (e) MSL pressure at 1800 UTC. (f) Geopotential height at 500 hPa on 13 June at 1800 UTC. (g) (right) 4-day back trajectories for arrival pressures of 500, 700, 850 and 975 hPa at 19 UTC and (left) zoom of the arrival.

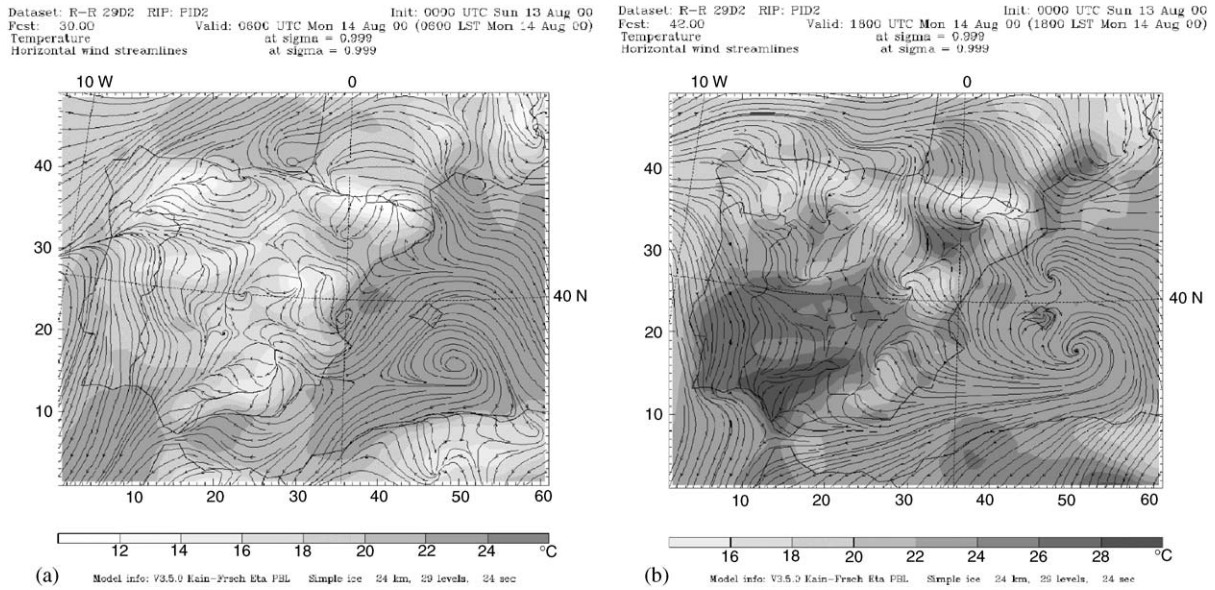

Fig. 8. Surface streamlines and temperature for the 14 August 2000 over domain D2. (a) 06 UTC. (b) 18 UTC.

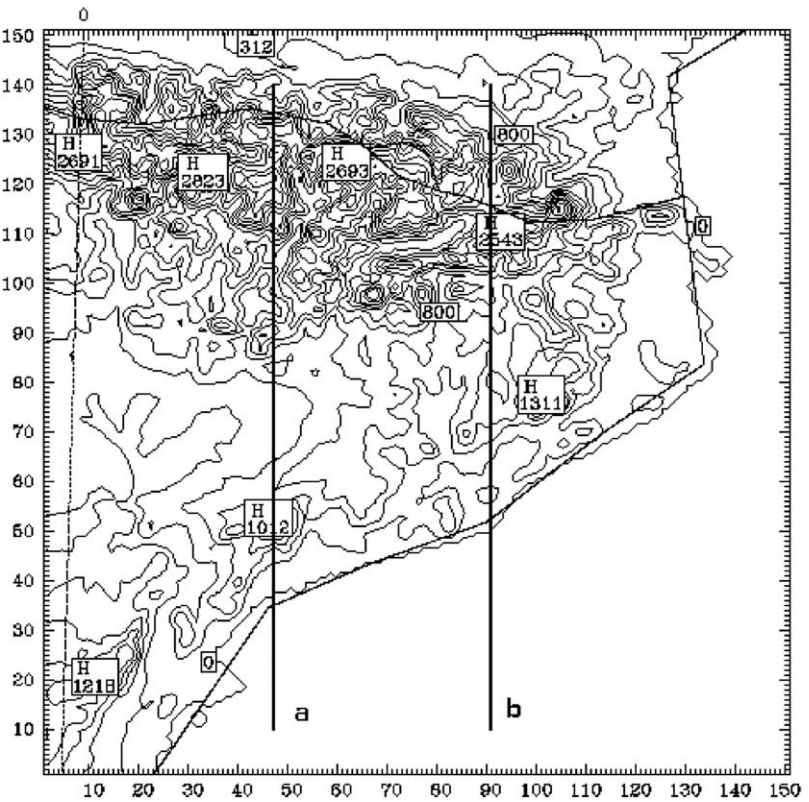

Fig. 9. D4 domain for simulation with MM5. Lines indicate the position of the vertical cross sections in Fig. 10.

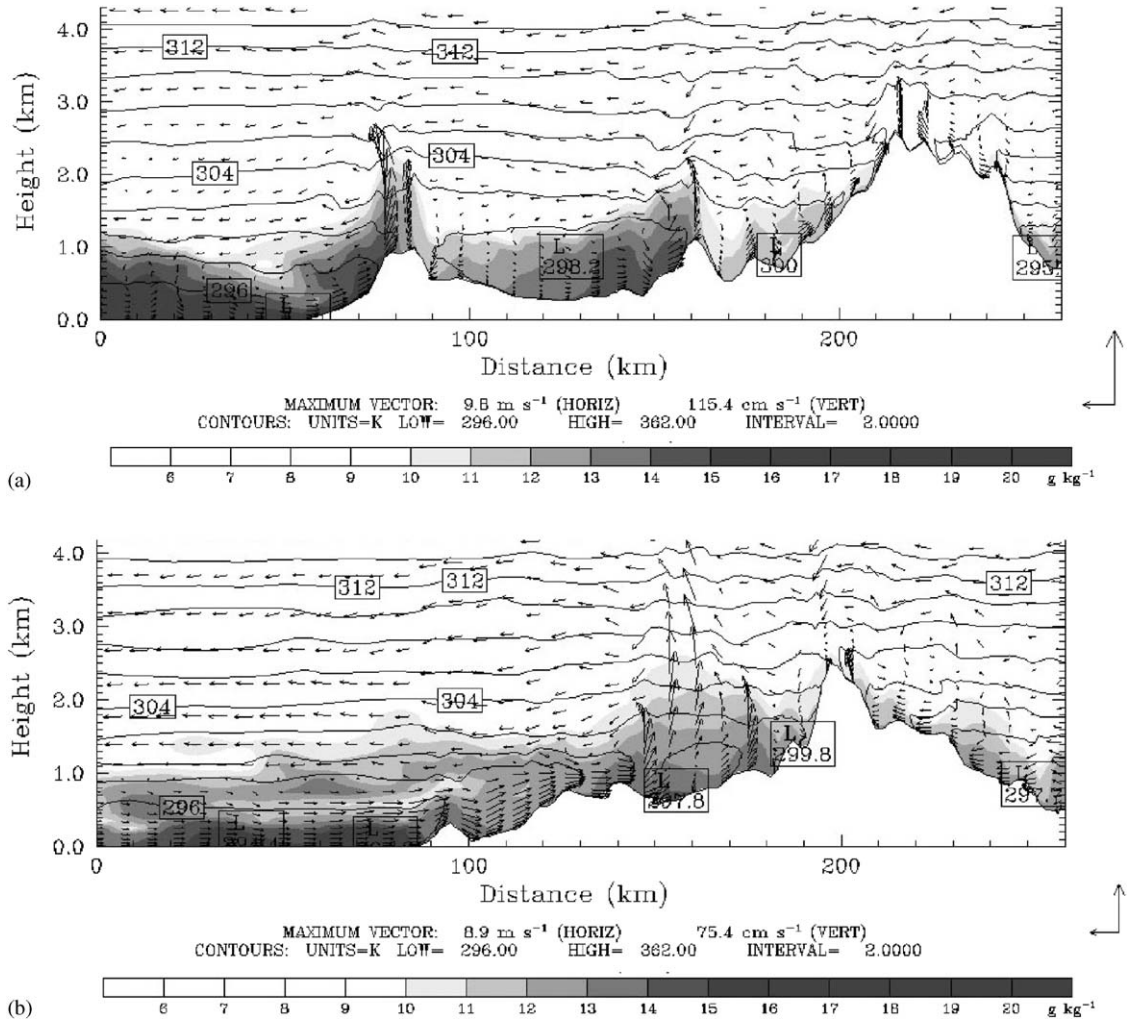

Fig. 10. Vertical cross sections of the wind field, potential temperature and mixing ratio on 14 August 2000. (a) Pyrenees–Tarragona cross section at 11 UTC. (b) Pyrenees–Barcelona cross section at 16 UTC.

morning followed by the sinking of its capping inversion during the afternoon. Lidar profiles in Section 4 follow this same pattern (see Figs. 4a–c, 5a–c, 6a). In addition, sea breezes introduce cool and stable air over the coast. As the column of air advects downwind and warms, the temperature difference between the air and the ground lessens. As a result, the heat flux at the ground decreases, the ML warms less rapidly, and the rise rate of the MH is reduced (Stull, 1988). Generally, TIBL's do not extend all the way to the top of the marine air associated with the intruding air mass, so the remainder of the cool air mass above the TIBL and below the return flows, acts as well as a barrier for the TIBL vertical development.

In Section 4, synoptic back trajectories (although they do not depict the precise movement of the air masses) and radiosoundings helped to identify and describe the main synoptic and large mesoscale features involved in the formation of the re-circulation layers detected by the lidar. Anticyclonic circulations with general and compensatory subsidence over the WMB were observed in all the episodes. Injections of polluted air masses from the Tarragona coastal mountains of the northeastern IP into the return flow account for the layers detected between 1500 and 2500 m in Sections 4.2 and 4.3 as depicted by the 850 hPa back trajectory (Figs. 4 and 5). The detection of some upper polluted layers (2500–4000 m) may be attributed to the effect of the Iberian Thermal low (see Figs. 3a and e) or to long range transport of aerosols (see Figs. 4c and f).

Maximum backscatter coefficients ranged from 1×10^{-6} to 2×10^{-6} $(\mathrm{m\,sr})^{-1}$ at the wavelength of

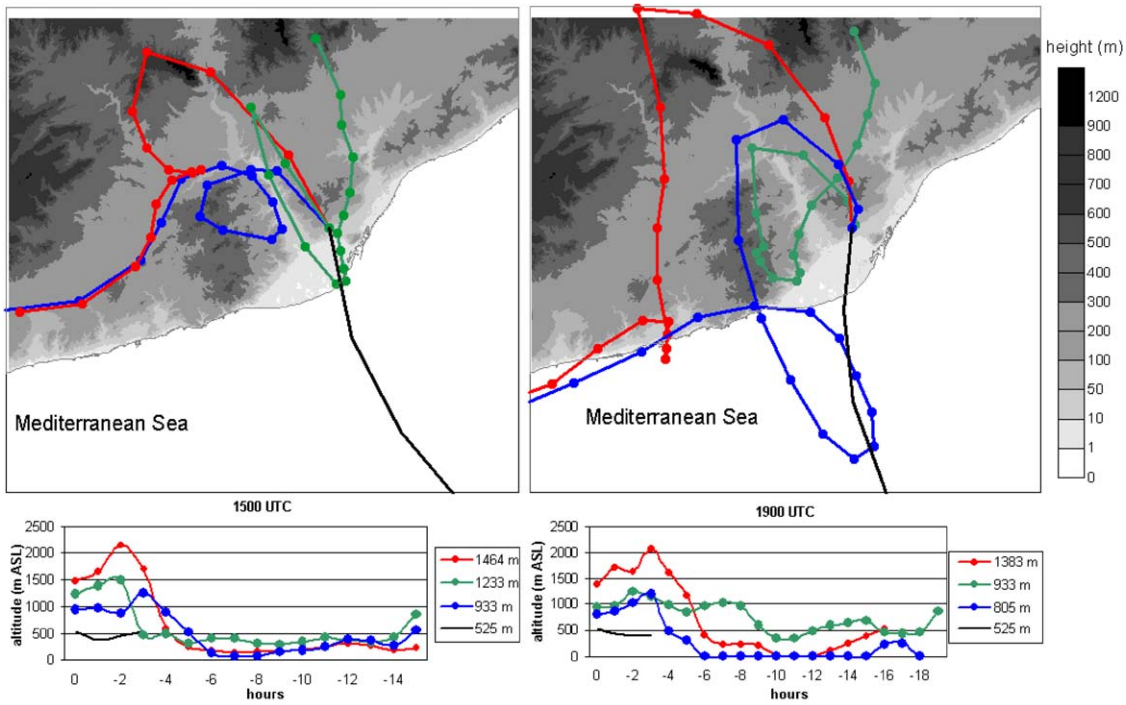

Fig. 11. Hysplit kinematic back trajectories arriving over the lidar station on 14 August 2000 from the MM5 high resolution domain (D4; 2 km; 29 σ-layers) over the orographic map of the Barcelona area. (left) at 15 UTC and (right) at 19 UTC.

1064 nm. Assuming a lidar ratio of 30 sr, AOD's of the re-circulation layers above the ML ranged from 0.016 (Fig. 4g) to 0.073 (Fig. 4j).

On 14 June 2002 (Section 4.4) the lidar probed simultaneously stratified aerosol layers from regional re-circulations below 3000 m and upper plume-like structures of Saharan dust. The top of the main Saharan dust layers reached altitudes up to 5500 m. Traces of dust were found up to 7000 m. A lidar ratio of 60 sr was assumed for the Saharan dust layers which in combination with the re-circulation layers yielded AOD's of 0.047 and 0.046 (Figs. 6b and c). Ansmann et al. (2003) found AOD's above 1000 m height ranging from 0.07 to 0.29 under strong Saharan dust intrusion over Barcelona.

High resolution modelling of the 14 August 2000 with PSU/NCAR Mesoscale Model 5 (MM5) described the mesoscale phenomena driving the circulations within the eastern IP and the WMB under a stagnant situation. Back trajectories from the highest resolution domain (D4; 2 km) described the main local pathways and injections of the polluted air masses detected by the lidar at 1500 UTC and 19 UTC up to 1400–1500 m (Fig. 11). Onshore flows start around 8–10 UTC and cease at 19 UTC. Air mass injections up to 2200 m are detected by the model. Compensatory subsidence is induced in their return flow towards the sea. Aerosol layers formed by injections at the coastal and pre-coastal mountain ranges at different times can be simultaneously detected between 800 and 1500 m over the lidar station. Strength and direction of sea breezes and return flows, and compensatory subsidence depend on the prevailing synoptic and large mesoscale conditions and account for the heights of the detected aerosol layers over Barcelona.

Combination of lidar data with synoptic analysis and numerical weather prediction models are powerful tools to study atmospheric circulations of aerosols and boundary layer structure at a regional to local scale pointing out the specificity of a particular area. Further work will be performed with the recently upgraded UPC mobile lidar system, integrating a Raman channel and scanning capabilities to focus on the optical properties of these frequent re-circulation aerosol layers.

Acknowledgements

This work was supported by the EARLINET project from the European Commission under grant EVR1-CT1999-40003 and CICYT REN2003-09753-C02.

The authors gratefully acknowledge the following organizations: the NOAA Air Resources Laboratory (ARL) for the provision of READY website (http://www.arl.noaa.gov/ready.html) and the HYSPLIT trajectory model, the Spanish Meteorological Institute (INM) for providing data from the ECMWF and the German Weather Service for the atmospheric back trajectories. Simulations were run on an HP Exemplar V2500 belonging to the Supercomputing Center of Catalonia (CESCA). ESA and MCYT are thanked, respectively, for the external postdoctoral fellowship and the Ramón y Cajal position hold by M. Sicard.

References

Ansmann, A., Bösenberg, J., Chaikovsky, A., Comerón, A., Eckhardt, S., Eixmann, R., Freudenthaler, V., Ginoux, P., Komguem, L., Linné, H., López Márquez, M.A., Matthias, V., Mattis, I., Mitev, V., Müller, D., Music, S., Nickovic, S., Pelon, J., Sauvage, L., Sobolewsky, P., Srivastava, M.K., Stohl, A., Torres, O., Vaughan, G., Wandinger, U., Wiegner, M., 2003. Long-range transport of Saharan dust to northern Europe: the 11–16 October 2001 outbreak observed with EARLINET. Journal of Geophysical Research 108 (D24), 4783, doi:10.1029/2003JD003757.

Baldasano, J.M., Cremades, L., Soriano, C., 1994. Circulation of air pollutants over the Barcelona geographical area in summer. Proceedings of Sixth European Symposium Physico-Chemical Behaviour of Atmospheric Pollutants, Varese (Italy), 18–22 October, 1993. Report EUR 15609/1: 474–479.

Barros, N., Toll, I., Soriano, C., Jiménez, P., Borrego, C., Baldasano, J.M., 2003. Urban photochemical pollution in the Iberian peninsula: the Lisbon and Barcelona airsheds. Journal of the Air and Waste Management Association 53, 347–359.

Batchvarova, E., Cai, X., Gryning, S.E., Steyn, D., 1999. Modelling internal boundary layer development in a region with complex coastline. Boundary-Layer Meteorology 90, 1–20.

Beck, J.P., Kryzanowski, M., Koffi, B., 1999. Ozone in the European Union. The Consolidated Report. European Topic Centre Air Quality, Bilthoven, The Netherlands. European Commission, Office for Official Publication.

Boers, R., Eloranta, E.W., Coulter, R.L., 1984. Lidar observations of mixed layer dynamics: test of parametrized entrainment models of mixed layer growth rate. Journal of Climate and Applied Meteorology 23, 247–266.

Bösenberg, J., Ansmann, A., Baldasano, J.M., Balis, D., Böckmann, C., Calpini, B., Chaikovsky, A., Flamant, P., Hagard, A., Mitev, V., Papayannis, A., Pelon, J., Resendes, D., Schneider, J., Spinelli, N., Trickl, T., Vaughan, G., Visconti, G., Wiegner, M., 2001. EARLINET: A European Aerosol Research Lidar Network. In: Dabas, A., Loth, C., Pelon, J. (Eds.), Advances in Laser Remote Sensing, Selected papers presented at the 20th International Laser Radar Conference (ILRC), Vichy, France, 10–14 July 2000, pp. 155–158.

Bösenberg, J., Matthias, V., et al., 2003. EARLINET: A European Aerosol Research Lidar Network. Report 348, MPI-Report 337, Max-Planck-Institut für Meteorologie, Hamburg, 191pp.

Costa, M., Baldasano, J.M., 1996. Development of a source emission model for atmospheric pollutants of the Barcelona area. Atmospheric Environment 30A (2), 309–318.

Draxler, R.R., Hess, G.D., 1998. An overview of the Hysplit_4 modelling system for trajectories, dispersion, and deposition. Australian Meteorological Magazine 47, 295–308.

Dudhia, J., 1993. A non-hydrostatic version of the Penn State-NCAR mesoscale model: Validation tests and simulation of an Atlantic cyclone and cold front. Monthly Weather Review 121, 1493–1513.

Dudhia, J., Gill, D., Manning, K., Wang, W., Bruyere, C., 2004. PSU/NCAR Mesoscale Modeling System Tutorial Class Notes and User's Guide: MM5 Modeling System Version 3 (http://www.mmm.ucar.edu/mm5/documents/tutorial-v3-notes.html).

Dupont, E., Pelon, J., Flamant, C., 1994. Study of the moist convective boundary layer by backscatter lidar. Boundary-layer Meteorology 69, 1–25.

European Commission, 1999. Ozone Position Paper. Office for Official Publications of the European Communities, Luxembourg, 173pp.

Fenger, J., Hertel, O., Palmgren, F., 1998. Urban Air Pollution—European Aspects, IV Series: Environmental Pollution. Kluwer Academic Publishers, Dordrecht, Netherlands, 492pp.

Fernald, F.G., 1984. Analysis of atmospheric lidar observations: some comments. Applied Optics 23, 652–653.

Gangoiti, G., Millán, M.M., Salvador, R., Mantilla, E., 2001. Long-range transport and re-circulation of pollutants in the western Mediterranean during the project regional cycles of air pollution in the west-central Mediterranean area. Atmospheric Environment 35, 6267–6276.

Jacobson, M.Z., 2001. Global direct radiative forcing due to multicomponent anthropogenic and natural aerosols. Journal of Geophysical Research 106, 1551–1568.

Janjic, Z.I., 1994. The step-mountain eta coordinate model: further development of the convection, viscous sublayer, and turbulent closure schemes. Monthly Weather Review 122, 927–945.

Jorba, O., Gassó, S., Baldasano, J.M., 2003. Regional circulations within the Iberian Peninsula east coast. 26th International Technical Meeting of NATO-CCMS on Air Pollution Modelling and its Application, Istanbul, Turkey, 26–30 May.

Jorba, O., Pérez, C., Rocadenbosch, F., Baldasano, J.M., 2004. Cluster analysis of 4-day back trajectories arriving in the Barcelona region from 1997 to 2002. Journal of Applied Meteorology, in press.

Kain, J.S., Fritsch, J.M., 1993. Convective parameterisation for mesoscale models: the Kain-Fritsch scheme. The Representation of Cumulus Convection in Numerical Models. Meteorological Monographs 46, American Meteorological Society, 165–170.

Klett, J.D., 1981. Stable analytical inversion solution for processing lidar returns. Applied Optics 20, 211–220.

Kolev, I., Skakalova, T., Grogorov, I., 2000. Lidar measurement of aerosol extinction profile in a coastal zone of the

Bulgarian Black Sea. Atmospheric Environment 34 (22), 3813–3822.

Matthias, V., Bösenberg, J., 2002. Aerosol climatology for the planetary boundary layer derived from regular lidar measurements. Atmospheric Research 63, 221–245.

Mattis, I., Ansmann, A., Müller, D., Wandinger, U., Althausen, D., 2002. Dualwavelength Raman lidar observations of the extinction-to-backscatter ratio of Saharan dust. Geophysical Research Letters 29 (9), 1306, doi:10.1029/2002GL014721.

Menut, L., Flamant, C., Pelon, J., Flamant, P.H., 1999. Urban boundary-layer height determination from lidar measurements over the Paris area. Applied Optics 38 (6), 945–954.

Millán, M.M., Artiñano, B., Alonso, L., Castro, M., Fernandez-Patier, R., Goberna, J., 1992. Mesometeorological cycles of air pollution in the Iberian Peninsula. Air Pollution Research Report 44, Commission of the European Communities, Brussels, Belgium, 219pp.

Millán, M., Salvador, R., Mantilla, E., Artiñano, B., 1996. Meteorology and photochemical air pollution in Southern Europe: experimental results from EC research projects. Atmospheric Environment 30 (12), 1909–1924.

Millán, M.M., Salvador, R., Mantilla, E., 1997. Photooxidant dynamics in the Mediterranean basin in summer: results from European research projects. Journal of Geophysical Research 102 (D7), 8811–8823.

Millán, M.M., Mantilla, E., Salvador, R., Carratal!a, A., Sanz, M.J., Alonso, L., Gangoiti, G., Navazo, M., 2000. Ozone cycles in the western Mediterranean basin: interpretation of monitoring data in complex coastal terrain. Journal of Applied Meteorology 39, 487–508.

Millán, M.M., Sanz, M.J., Salvador, R., Mantilla, E., 2002. Atmospheric dynamics and ozone cycles related to nitrogen deposition in the western Mediterranean. Environmental Pollution 118, 167–186.

Müller, D., Mattis, I., Wandinger, U., Althausen, D., Ansmann, A., Dubovik, O., Eckhardt, S., Stohl, A., 2003. Saharan dust over a central European EARLINET-AERONET site: combined observations with Raman lidar and Sun photometer, Journal of Geophysical Research 108(D12), 4345, doi:10.1029/2002JD002918.

Nickovic, S., Kallos, G., Papadopoulos, A., Kakaliagou, O., 2001. A model for prediction of desert dust cycle in the atmosphere. Journal of Geophysical Research 106, 18113–18129.

Querol, X., Alastuey, A., Puicercus, J.A., Mantilla, E., Ruiz, C.R., Lopez-Soler, A., Plana, F., Juan, R., 1998. Seasonal evolution of suspended particles around a large coal-fired power station: chemical characterisation. Atmospheric Environment 32 (11), 719–731.

Rocadenbosch, F., Soriano, C., Comerón, A., Baldasano, J.M., Rodríguez, A., Muñoz, C., García-Vizcaíno, D., 2001. 3D scanning portable backscatter lidar platform for atmospheric remote sensing: performance and architecture overview. Proceedings of the SPIE 4168, 158–169.

Rodríguez, S., Querol, X., Alastuey, A., Kallos, G., Kakaliagou, O., 2001. Saharan dust contributions to PM10 and TSP levels in southern and eastern Spain. Atmospheric Environment 35, 2433–2447.

Rodríguez, S., Querol, X., Alastuey, A., Mantilla, E., 2002. Origin of high summer PM10 and TSP concentrations at rural sites in eastern Spain. Atmospheric Environment 36, 3101–3112.

Sasano, Y., Nakane, H., 1984. Significance of the extinction/backscatter ratio and the boundary value term in the solution for the two-component lidar equation. Applied Optics 23, 11–12.

Sicard, M., Pérez, C., Comerón, A., Baldasano, J.M., Rocadenbosch, F., 2003. Determination of the mixing layer height from regular lidar measurements in the Barcelona Area. Proceedings of the SPIE 5235, 505–516.

Skakalova, T.S., Savov, P.B., Grigorov, I.V., Kolev, I.N., 2003. Lidar observation of breeze structure during the transition periods at the southern Bulgarian Black Sea coast. Atmospheric Environment 37, 299–311.

Soriano, C., Baldasano, J.M., 1998. Study of the land-sea interface in the Barcelona area with lidar data and meteorological models. In: Brebbia, C.A. (Ed.), Environmental Coastal Regions. Computational Mechanics Publications, Wessex Institute of Technology, UK, pp. 135–142.

Soriano, C., Baldasano, J.M., Buttler, W.T., Moore, K., 2001. Circulatory patterns of air pollutants within the Barcelona air basin in a summertime situation: lidar and numerical approaches. Boundary-Layer Meteorology 98 (1), 33–55.

Stull, R.B., 1988. An Introduction to Boundary Layer Meteorology. Kluwer Academic Publishers, Dordrecht, 670pp.

Toll, I., Baldasano, J.M., 2000. Photochemical modeling of the Barcelona area with highly disaggregated anthropogenic and biogenic emissions. Atmospheric Environment 34 (19), 3069–3084.

Tudurí, E., Romero, R., López, L., García, E., Sánchez, J.L., Ramis, C., 2003. The 14 July 2001 hailstorm in northeastern Spain: diagnosis of the meteorological situation. Atmospheric Research 67–68, 541–558.

Wakimoto, R.M., McElroy, J.L., 1986. Lidar observation of elevated pollution layers over Los Angeles. Journal of Climate and Applied Meteorology 25, 1583–1599.